PHYSICAL REVIEW A VOLUME 40, NUMBER 3 AUGUST 1, 1989

Non-Markovian dynamics of electron-molecule collision complexes

Hernán Estrada
Departamento de Fisica, Universidad Nacional de Colombia, Bogotá, Colombia

Wolfgang Domcke
Institut für Physikalische und Theoretische Chemie, Technische Universität München, D-8046 Garching, Federal Republic of Germany
(Received 13 February 1989)

The time-dependent description of the dynamics of electron-molecule collision complexes is outlined within the framework of Feshbach's projection-operator formalism. It is shown that the equation of motion for the quantum-mechanical wave packet representing the collision complex contains effective-potential terms which are nonlocal as well as non-Markovian, that is, the time development depends on the previous history of the system. The space-time integro-differential equation of motion is explicitly (numerically) solved for a class of simple models using expansions into complete sets of functions in both space and time. The exact wave-packet dynamics is compared with the results obtained in the local-complex-potential approximation, which corresponds to the Markovian approximation for the decay dynamics. The concepts and numerical methods are illustrated for a model of the well-known $^2\Pi_g$ shape resonance in electron-N_2 scattering, where the boomerang effect is reproduced. For a model of a p-wave shape resonance near threshold, novel qualitative effects are revealed, namely, nonmonotonic electronic decay (recapture of electrons from the continuum) as well as strong frictional effects in the vibrational motion. The time-dependent description of virtual-state threshold effects in s-wave scattering is also briefly considered.

I. INTRODUCTION

Short-lived autodetaching electronic states of molecular anions (resonances) play a crucial role as intermediates in a variety of elementary collision processes such as vibrationally inelastic electron-molecule scattering, dissociative attachment, and associative detachment.[1,2] It has been recognized for a long time that the description of these phenomena generally requires a nonperturbative treatment of the electron-molecule collision process. Moreover, the familiar close-coupling expansion in terms of target vibrational states, besides being unable to account for reactive processes, becomes slowly convergent and thus inefficient in the presence of resonances.[3,4] Therefore, models or computational techniques which treat explicitly the nuclear dynamics in electronic resonance states are appropriate. Among these the formulations based on the projection-operator approach of Feshbach[5] or the R-matrix method[6] have found the most widespread application.[7–15]

In the projection-operator formulation[7–10,13,15] *diabatic*[16,17] electronic basis states are employed to formulate the collision problem. In the simplest case of an isolated single-channel resonance (in the fixed-nuclei limit) the electronic Hilbert space is spanned by a discrete electronic state $|\phi_d\rangle$ and a scattering continuum $|\phi_{\mathbf{k}}\rangle$ with associated projectors

$$Q=|\phi_d\rangle\langle\phi_d| \ , \tag{1.1a}$$

$$P=\int k\, dk\, d\Omega_{\mathbf{k}}|\phi_{\mathbf{k}}\rangle\langle\phi_{\mathbf{k}}| \ , \tag{1.1b}$$

such that

$$P+Q=1, \quad PQ=0 \ . \tag{1.2}$$

As is well known, the dynamical problem (that is, electronic decay as well as vibration and dissociation of the collision complex) reduces to the treatment of nuclear dynamics in a complex, energy-dependent, and nonlocal effective potential.[7–10,13,15] In most applications this nonlocal effective potential has been replaced by a *local* complex potential which can be derived by neglecting the energy dependence of the exact effective potential and using the closure property of the vibrational states of the target molecule.[8,13,15,18,19]

The present work is intended as a first step towards the exploration of the *time-dependent* view of the dynamics of electron-molecule collision complexes. Time-dependent wave-packet methods are nowadays becoming increasingly popular in the field of molecular reaction dynamics; see, e.g., Refs. 20–28. Attractive features of time-dependent wave-packet formulations are the ease of interpretation and gain of intuitive insight, as well as the possibility of introducing efficient semiclassical approximation methods for multidimensional problems.[21–23,29,30]

McCurdy and Turner[31] have lucidly discussed the advantages of semiclassical Gaussian wave-packet propagation methods[21,22] for short-lived resonance states within the framework of the local-complex-potential (LCP) model. As will be shown below, the exact treatment of the problem within the projection-operator formalism yields a time-dependent equation of motion for the nuclear dynamics with an effective-potential term which is complex, nonlocal in space, as well as nonlocal in time, and thus contains memory effects. The dynamics of electron-molecule collision complexes is thus a *non-Markovian process* in the exact description. The LCP approximation corresponds to the Markov approximation for the decay dynamics.

Owing to the complexity of the equation of motion for wave packets in short-lived anions as compared to the usual time-dependent Schrödinger equation, the interpretive aspect of the time-dependent description is particularly important. Our first goal is therefore to obtain exact (numerical) solutions of the non-Markovian equation of motion for simple, but fairly general, models of electron-molecule-scattering resonances. We have developed an efficient numerical scheme to solve the space-time integro-differential equation of motion for this class of models. These exact results allow us to identify characteristic non-Markovian effects in electron-molecule collision complexes by comparison with results obtained in the LCP approximation. Some first results of the present work have been presented in Ref. 32.

II. GENERAL THEORY

A. The Hamiltonian

In this work we are primarily concerned with isolated shape resonances in electron-molecule scattering, although, as will be shown below, virtual-state effects in s-wave scattering are also included in the present formulation. We shall work within a diabatic electronic representation consisting of a single discrete state $|\phi_d\rangle$ and an orthogonal background scattering continuum $|\phi_{\mathbf{k}}\rangle$ as discussed in the Introduction. The explicit construction of these diabatic electronic basis states has been extensively discussed for the representative electron-molecule collision systems $e+\mathrm{N}_2(^2\Pi_g)$, $e+\mathrm{H}_2(^2\Sigma_u^+)$, $e+\mathrm{F}_2(^2\Sigma_u^+)$, and $e+\mathrm{HCl}(^2\Sigma)$, employing either finite-basis-set methods[33–37] or scattering-theoretic methods.[38–40] It should be stressed that the $|\phi_{\mathbf{k}}\rangle$ are not simply plane waves, but rather exact (energy-normalized) background scattering states which have to be constructed by solving the fixed-nuclei electron-molecule scattering problem in P space.[38,39] The Hamiltonian is thus written as (atomic units are assumed throughout)

$$\begin{aligned} H = {} & |\phi_d\rangle[T_N+V_d(R)]\langle\phi_d| \\ & + \int k\,dk d\Omega_{\mathbf{k}}|\phi_{\mathbf{k}}\rangle[T_N+V_0(R)+k^2/2]\langle\phi_{\mathbf{k}}| \\ & + \int k\,dk d\Omega_{\mathbf{k}}(|\phi_d\rangle V_{d\mathbf{k}}\langle\phi_{\mathbf{k}}|+\mathrm{H.c.}) \,. \end{aligned} \tag{2.1}$$

Here T_N is the kinetic-energy operator of nuclear motion, $V_0(R)$ the electronic potential energy of the target molecule as a function of internuclear distance R, and $V_d(R)$ the potential energy of the discrete electronic state, which is coupled to the electronic continuum via the coupling matrix element $V_{d\mathbf{k}}$, which may depend on R in general. For the sake of simplicity we restrict ourselves to diatomic target molecules and suppress the rotational degrees of freedom, that is, T_N in Eq. (2.1) is taken as the radial kinetic-energy operator

$$T_N = -(2\mu)^{-1}\frac{d^2}{dR^2} \,, \tag{2.2}$$

where μ is the reduced mass of the target molecule.

The basic assumption of this formulation is that the action of T_N on the wave functions of the diabatic electronic basis states $|\phi_d\rangle, |\phi_{\mathbf{k}}\rangle$ is negligible. In particular, we neglect direct continuum-continuum couplings via T_N (note that the electronic continuum is exactly prediagonalized in the fixed-nuclei approximation). It has been shown that these assumptions are well justified for low-energy resonant electron-molecule scattering and that the resulting theory is able to describe quantitatively the experimental data for a variety of electron-molecule collision systems.[13,15,34,41,42]

B. Equation of motion and scattering amplitudes

The time-dependent description of the dynamics of electron-molecule collision complexes is obtained from the Hamiltonian (2.1) and the time-dependent Schrödinger equation

$$i\frac{\partial}{\partial t}|\Psi(t)\rangle\rangle = H|\Psi(t)\rangle\rangle \,, \tag{2.3}$$

where $|\Psi(t)\rangle\rangle$ is the full time-dependent state vector of the collision system. The double ket is used to denote a state vector in the combined Hilbert spaces of electronic and nuclear motion.

Defining the electronically projected states

$$|\psi_d(t)\rangle = \langle\phi_d|\Psi(t)\rangle\rangle \,, \tag{2.4a}$$

$$|\psi_{\mathbf{k}}(t)\rangle = \langle\phi_{\mathbf{k}}|\Psi(t)\rangle\rangle \,, \tag{2.4b}$$

one obtains from (2.1) and (2.3) the coupled equations

$$i\frac{\partial}{\partial t}|\psi_d(t)\rangle = \tilde{H}_d|\psi_d(t)\rangle + \int k\,dk\,d\Omega_{\mathbf{k}}V_{d\mathbf{k}}|\psi_{\mathbf{k}}(t)\rangle \,, \tag{2.5a}$$

$$i\frac{\partial}{\partial t}|\psi_{\mathbf{k}}(t)\rangle = (\tilde{H}_0+k^2/2)|\psi_{\mathbf{k}}(t)\rangle + V_{\mathbf{k}d}|\psi_d(t)\rangle \,, \tag{2.5b}$$

where

$$\tilde{H}_0 = T_N + V_0(R) \,, \tag{2.6a}$$

$$\tilde{H}_d = T_N + V_d(R) \tag{2.6b}$$

are the vibrational Hamiltonians of the target state and the discrete state, respectively.

Coupled equations of similar structure are commonly encountered in semiclassical models of detachment or ion-neutralization processes where the nuclear motion is assumed to follow a classical trajectory, rendering the Hamiltonian of the electronic subsystem time dependent.[43–47] Here, in contrast, we treat the nuclear motion fully quantum mechanically and solve the time-dependent Schrödinger equation for a time-independent Hamiltonian.

As a consequence of the absence of direct continuum-continuum couplings, Eq. (2.5b) can be formally solved as an inhomogeneous first-order differential equation, yielding

$$|\psi_{\mathbf{k}}(t)\rangle = e^{-i(\tilde{H}_0+k^2/2)t}\left[|\psi_{\mathbf{k}}(0)\rangle + \frac{1}{i}\int_0^t dt' e^{i(\tilde{H}_0+k^2/2)t'} V_{\mathbf{k}d}|\psi_d(t')\rangle\right] . \tag{2.7}$$

Insertion of (2.7) into Eq. (2.5a) yields

$$i\frac{\partial}{\partial t}|\psi_d(t)\rangle = \tilde{H}_d|\psi_d(t)\rangle + \frac{1}{i}\int_0^t dt' \tilde{F}(t-t')|\psi_d(t')\rangle + |S(t)\rangle , \tag{2.8}$$

where

$$\tilde{F}(t) = \int k\, dk\, d\Omega_{\mathbf{k}} V_{d\mathbf{k}} e^{-i(\tilde{H}_0+k^2/2)t} V_{\mathbf{k}d} , \tag{2.9}$$

$$|S(t)\rangle = \int k\, dk\, d\Omega_{\mathbf{k}} V_{d\mathbf{k}} e^{-i(\tilde{H}_0+k^2/2)t}|\psi_{\mathbf{k}}(0)\rangle . \tag{2.10}$$

It is obvious from Eq. (2.8) that the operator $\tilde{F}(t)$ accounts for the effect of the discrete-continuum coupling on the nuclear motion in the discrete state. The inhomogeneity $|S(t)\rangle$ in Eq. (2.8) may be called a "source term" and depends on the initial condition dictated by the experiment under consideration.

For resonant electron-molecule collisions the appropriate initial condition is

$$|\psi_d(0)\rangle = V_{d\mathbf{k}_i}|v\rangle ; \quad |\psi_{\mathbf{k}}(0)\rangle = 0 \tag{2.11}$$

where $\mathbf{k}_i$ denotes the momentum of the incoming electron and $|v\rangle$ the vibrational state of the target molecule. The matrix element $V_{d\mathbf{k}_i}$ in Eq. (2.11) has the obvious meaning of an "entrance amplitude" for the electron. The time $t=0$ corresponds to the first capture of the electron into the resonance state. This event "sets the clock" for the ensuing dynamical evolution of the collision complex. According to Eq. (2.11) the source term (2.10) vanishes for electron-molecule collision processes. It vanishes also for the reverse process, that is, electron collisional detachment,[45–47] and thus need not be considered any further.

Adopting coordinate-space representation in the Hilbert space of nuclear motion

$$\psi_d(R,t) = \langle R|\psi_d(t)\rangle ,$$

we finally have the basic equation of motion for the wave packet representing the collision complex

$$i\frac{\partial}{\partial t}\psi_d(R,t) = \tilde{H}_d\psi_d(R,t) + \frac{1}{i}\int_0^\infty dR' \int_0^t dt' F(R,R';t-t')\psi_d(R',t') , \tag{2.12}$$

with

$$F(R,R';t) = \int k\, dk\, d\Omega_{\mathbf{k}} e^{-i(k^2/2)t} V_{d\mathbf{k}}(R) K_0(R,R';t) V_{\mathbf{k}d}(R') . \tag{2.13}$$

Here,

$$K_0(R,R';t) = \langle R|e^{-i\tilde{H}_0 t}|R'\rangle \tag{2.14}$$

is the Feynman propagator[48] for nuclear motion in the target molecule. The dependence of the discrete-continuum coupling element $V_{d\mathbf{k}}$ on the internuclear distance has been displayed explicitly for clarity. The initial condition (2.11), which complements the equation of motion, is written in coordinate-space representation as

$$\psi_d(R,t=0) = V_{d\mathbf{k}_i}(R)\chi_v(R) , \tag{2.15}$$

where $\chi_v(R)$ denotes the vibrational wave function of the target molecule.

The integral kernel $F(R,R';t-t')$, which accounts for the effects of the coupling of the discrete state with the continuum and thus the decay of the resonance, is seen to be complex and nonlocal in space as well as in time. The time evolution of the wave packet $\psi_d(R,t)$ is thus determined by the value of ψ_d at all previous times since the formation of the collision complex, that is, the evolving wave packet possesses a memory on its history. The integral kernel $F(R,R';t-t')$ will henceforth be called the "memory kernel" of the equation of motion. The existence of a memory implies that the wave-packet dynamics of the collision complex is *non-Markovian*. Aspects of non-Markovian dynamics have been discussed for the related, though simpler, problem of a rigorous treatment of the Wigner-Weisskopf model of atomic fluorescence.[49–52] Non-Markovian equations of motion (for reduced density matrices or correlation functions) play also a central role in nonequilbrium statistical mechanics.[53–55] The basic properties of the memory kernel $F(R,R';t-t')$ for electron-molecule collision complexes will be discussed in Sec. III below.

The physical relevance of the time-dependent description outlined so far rests on the fact that the time-dependent wave packet $\psi_d(R,t)$ contains the *complete* information on all resonant scattering amplitudes. The T-matrix element for elastic and vibrationally inelastic scattering, $T_{v',v}$ is given by

$$T_{v'v}(E) = \frac{1}{i}\int_0^\infty dt\, e^{iEt}\int_0^\infty dR\, \chi^*_{v'}(R)V^*_{d\mathbf{k}_f}(R)\psi_d(R,t) \tag{2.16}$$

where $\mathbf{k}_f$ denotes the final asymptotic momentum of the scattered electron. For collision systems where the dissociative attachment channel exists, the corresponding T-matrix element is given by

$$T_{\mathrm{DA}}(E) = (K/2\pi\mu)^{1/2}\lim_{R\to\infty} e^{-iKR}\int_0^\infty dt\, e^{iEt}\psi_d(R,t) , \tag{2.17}$$

where K is the relative momentum of the dissociating fragments. The corresponding integral cross sections are given by

$$\sigma_{v'v}(E)=\frac{4\pi^3}{k_i^2}\nu|T_{v'v}(E)|^2 \tag{2.18}$$

and

$$\sigma_{\mathrm{DA}}(E)=\frac{4\pi^3}{k_i^2}\nu|T_{\mathrm{DA}}(E)|^2 , \tag{2.19}$$

respectively, where ν counts the spatial degeneracy of the resonance state.

The physical interpretation of the scattering amplitudes (2.16) and (2.17) is rather obvious. The $v\rightarrow v'$ inelastic scattering amplitude is obtained by projecting the wave packet $\psi_d(R,t)$ onto the final vibrational wave function $\chi_{v'}(R)$, multiplied by the "exit amplitude" $V_{d\mathbf{k}_f}$, followed by Laplace transformation, which projects on the correct total energy E. The component of $\psi_d(R,t)$ which survives for $R\rightarrow\infty$ yields, after Laplace transformation, directly the amplitude of dissociative attachment at total energy E. The wave packet $\psi_d(R,t)$, although not directly accessible to experimental observation, is thus a physically relevant entity in that it carries the information on observable quantities.

The connection of the time-dependent formulation with the familiar time-independent projection-operator formalism[7–10,13,15] is given by Laplace transformation. Defining the time-independent wave function $\psi_{d,E}(R)$ for total energy E as

$$\psi_{d,E}(R)=\frac{1}{i}\int_0^{\infty}dt\, e^{iEt}\psi_d(R,t), \tag{2.20}$$

we find that $\psi_{d,E}$ satisfies the basic equation of the time-independent formalism[7–9]

$$[E-T_N-V_d(R)]\psi_{d,E}(R)-\int_0^{\infty}dR'F(R,R';E)\psi_{d,E}(R') = V_{d\mathbf{k}_i}(R)\chi_v(R) , \tag{2.21}$$

with

$$\begin{aligned}F(R,R';E)&=\frac{1}{i}\int_0^{\infty}dt\, e^{iEt}F(R,R';t)\\ &=\int k'dk'd\Omega_{\mathbf{k}'}V_{d\mathbf{k}'}(R)\\ &\quad\times G_0^{(+)}\left[R,R';E-\frac{(k')^2}{2}\right]V_{d\mathbf{k}'}^{*}(R') ,\end{aligned} \tag{2.22}$$

where

$$\begin{aligned}G_0^{(+)}(E)&=\langle R|(E-\tilde{H}_0+i\eta)^{-1}|R'\rangle\\ &=\frac{1}{i}\int_0^{\infty}dt\, e^{iEt}K_0(R,R';t)\end{aligned} \tag{2.23}$$

is the Green's function for nuclear motion in the target molecule. $F(R,R';E)$ represents the complex, energy-dependent and nonlocal level-shift function of the time-independent projection-operator formalism.[7–9,15] It is thus obvious that the memory effects of the time-dependent formulation are reflected by the energy dependence of the effective potential in the time-independent formulation.

C. Local-complex-potential approximation

As mentioned in the Introduction, the energy-dependent and nonlocal level-shift function (2.22) is often replaced by a local complex level shift in practical applications of the theory. The approximate local complex potential can be derived from the general formalism,[8,13,15,18,19] but has also independently been introduced on grounds of heuristic arguments.[31,56–58] There exist, in fact, several LCP approximations which are not strictly equivalent.[59]

In the most commonly employed LCP approximation, $F(R,R';E)$ of Eq. (2.22) is replaced by the local and energy-independent complex level-shift function $F_L(R)$ (Refs. 13, 15, and 19),

$$F(R,R';E)\rightarrow F_L(R)\delta(R-R') , \tag{2.24a}$$

$$F_L(R)=\Delta_L(R)-\frac{i}{2}\Gamma_L(R) , \tag{2.24b}$$

$$\Gamma_L(R)=\Gamma(R,E_{\mathrm{res}}(R)) , \tag{2.24c}$$

$$\Delta_L(R)=\Delta(R,E_{\mathrm{res}}(R)) , \tag{2.24d}$$

where $\Gamma(R,E)$ and $\Delta(R,E)$ are defined by

$$\Gamma(R,E)=2\pi\int d\Omega_{\mathbf{k}}|V_{d\mathbf{k}}(R)|^2 , \tag{2.25a}$$

$$\Delta(R,E)=\mathrm{P}\frac{1}{2\pi}\int dE'\Gamma(R,E')/(E-E') , \tag{2.25b}$$

and the real resonance energy $E_{\mathrm{res}}(R)$ is defined by the implicit equation

$$E_{\mathrm{res}}(R)=V_d(R)-V_0(R)+\Delta(R,E_{\mathrm{res}}(R)) . \tag{2.26}$$

The corresponding memory kernel in the time-dependent formulation is obtained by inversion of Eq. (2.22)

$$F(R,R';t)=i\int_{-\infty}^{\infty}dE\frac{1}{2\pi}e^{-iEt}F(R,R';E) . \tag{2.27}$$

As a consequence of the energy independence of $F_L(R)$, the resulting memory kernel is proportional to a δ function in time, i.e.,

$$F(R,R';t-t') \rightarrow i\left[\Delta_L(R)-\frac{i}{2}\Gamma_L(R)\right]\delta(R-R')\delta(t-t') . \tag{2.28}$$

The LCP approximation removes thus both the nonlocality as well as the memory of the exact effective potential. The LCP approximation is seen to be a specific realization of a Markovian approximation to the original non-Markovian equation of motion.

With the approximation (2.28), the time-dependent equation of motion (2.12) becomes

$$i\frac{\partial}{\partial t}\psi_d(R,t)=\left[T_N+V_d(R)+\Delta_L(R)-\frac{i}{2}\Gamma_L(R)\right]\psi_d(R,t). \tag{2.29}$$

Clearly, the solution of the partial differential equation (2.29) is a much simpler task than the solution of the more exact integro-differential equation in space and time, Eq. (2.12). An illuminating discussion of the wave-packet dynamics described by Eq. (2.29) has been given by McCurdy and Turner for the example of the $^2\Pi_g$ shape resonance in $e+N_2$ scattering.[31] An essential objective of the present work is to obtain solutions to the exact equation of motion (2.12) and to compare these with the results of the LCP approximation. We thus wish to obtain insight into the effects of nonlocality and memory for representative models of electron-molecule collision complexes.

It is an important feature of the LCP approximation, apart from the simplification of the equation of motion, that it is sufficient to know the decay width Γ as a function of the single variable R, whereas Γ is needed as a function of the two variables R and E in the nonlocal formulation. If $\Gamma(R,E)$ is not given, as is typically the case in phenomenological applications of the theory,[31,56–58] an additional approximation is necessary, namely, the replacement of the electron-energy-dependent entry and exit amplitudes $V_{d\mathbf{k}_i}$ and $V_{d\mathbf{k}_f}$ in Eqs. (2.15) and (2.16) by energy-independent quantities. It has been shown that this additional approximation, which is not related to the actual dynamics of the collision complex, may introduce serious errors for resonances near threshold[34,60–62] or for deeply inelastic scattering, where the scattered electron is slow.[61] It is thus preferable to keep the correct energy dependence of the entry and exit amplitudes in the evaluation of the T-matrix elements, while obtaining $\psi_d(R,t)$ from the Markovian equation of motion (2.29). This improved approximation scheme has been termed the "semilocal" approximation.[61,62] In the present work the LCP approximation will be employed in the sense of the semilocal approximation.

III. SOLUTION OF THE EQUATION OF MOTION FOR MODEL SYSTEMS

A. Definition of the model

The solution of the integro-differential equation (2.12) is not a trivial problem, even in the simplest case of a single vibrational coordinate. As an initial step towards a general solution of this problem we consider the dynamics of models with certain simplifying features, such that very efficient numerical techniques can be employed to obtain the desired solutions.

The class of models to be considered here has been introduced previously for the study of various aspects of resonance and threshold effects in electron-molecule scattering.[63–68] In particular, a unified description of shape resonances,[59,61,64] virtual-state effects in s-wave scattering,[63,68] threshold peaks in electron scattering from polar molecules,[65,66] and Coulomb threshold effects in electron-ion scattering[67] has been developed on the basis of these models.

The most essential simplification is the assumption of harmonic potential-energy functions for the target electronic state and the discrete state. Introducing, for convenience, the dimensionless vibrational coordinate

$$Q=(\mu\omega)^{1/2}(R-R_0)\ , \tag{3.1}$$

where R_0 is the equilibrium distance of the target molecule and ω the harmonic vibrational frequency, we write

$$V_0(Q)=\tfrac{1}{2}\omega Q^2\ , \tag{3.2a}$$

$$V_d(Q)=\tfrac{1}{2}\omega Q^2+\varepsilon+\kappa Q\ , \tag{3.2b}$$

where ε represents the energy of the discrete electronic state relative to the target electronic state at $R=R_0$, and the parameter κ determines the shift δQ of the equilibrium geometry of the discrete state according to

$$\delta Q=-\kappa/\omega\ . \tag{3.3}$$

As usual, the range of Q is taken to be $(-\infty,\infty)$. We assume here, for simplicity, identical vibrational frequencies for V_0 and V_d. The harmonic approximation for V_d eliminates, of course, the possibility to describe the dissociative attachment process. A variety of applications has shown, however, that such harmonic models are useful to obtain insight into the dynamics of $v\rightarrow v'$ elastic and inelastic electron-molecule scattering.[63–68]

As a further, purely technical, simplification we assume that the width function $\Gamma(R,E)$ defined in Eq. (2.25a) can be taken to be independent of the internuclear distance. The width Γ is thus a function of energy only, which has been referred to as the $\Gamma(E)$ approximation.[9,69] The energy dependence of Γ [and thus the discrete-continuum coupling element $V_{d\mathbf{k}}$, see Eq. (2.25a)] is assumed to be given by Wigner's threshold law[70] at low energy and a suitable cutoff function for high energies. For the present purposes, $\Gamma(E)$ will be parametrized as

$$\Gamma(E)=A\,(E/B)^{l+1/2}e^{-E/B}\ , \tag{3.4}$$

where l represents the lowest partial wave into which the resonance can decay according to symmetry selection rules, A measures the overall strength of the discrete-continuum coupling, and B defines the high-energy cutoff which is required to guarantee the existence of $\Delta(E)$ in Eq. (2.25b).

The independence of $V_{d\mathbf{k}}$ of the vibrational coordinate Q allows us to cast the basic equations of Sec. II into a simplified form. First, it is seen that the entry and exit amplitudes in Eq. (2.16) may be taken out of the vibrational integral (sort of Condon approximation)

$$T_{v'v}(E)=V^*_{d\mathbf{k}_f}V_{d\mathbf{k}_i}\frac{1}{i}\int_0^\infty dt\,e^{iEt}\int_{-\infty}^{\infty}dQ\,\chi^*_{v'}(Q)\psi_d(Q,t)\ . \tag{3.5}$$

$\psi_d(Q,t)$ is then subject to the initial condition

$$\psi_d(Q,t=0)=\chi_v(Q)\ , \tag{3.6}$$

which is independent of the collision energy. Therefore, for a given v, *all* $v \rightarrow v'$ scattering amplitudes for *all* collision energies are obtained from the *single* wave packet $\psi_d(Q,t)$ with initial condition (3.6).

For the class of models defined by Eqs. (3.2) and (3.4) the memory kernel $F(Q,Q';t)$ can be given in closed form which renders the analysis of memory effects particularly transparent. Introducing the inverse Laplace transform of the width function

$$\Gamma(t)=\int_0^\infty \frac{dE}{2\pi}\Gamma(E)e^{-iEt} = \frac{AB}{\sqrt{\pi}}\frac{(2l+1)!!}{2^{l+2}}(1+iBt)^{-(l+3/2)} \quad (3.7)$$

and making use of the known propagator for the harmonic oscillator,[48] we have

$$F(Q,Q';t)=\Gamma(t)[2\pi i \sin(\omega t)]^{-1/2} \times \exp\left[\frac{i}{2\sin(\omega t)}\{[Q^2+(Q')^2]\cos(\omega t) - 2QQ'\}\right] . \quad (3.8)$$

Equations (3.7) and (3.8) exhibit explicitly the nonlocality as well as the memory of the integral kernel in the equation of motion for the present class of models.

The matrix representation of F in the basis of target vibrational states $\{|v\rangle\}$ is diagonal, with diagonal elements given by

$$F_{vv}(t)=\Gamma(t)e^{-i[v+1/2]\omega t} . \quad (3.9)$$

$F_{vv}(t)$ contains three characteristic time dependencies, namely, an oscillation with frequency $v\omega$, a short-time decay of $\Gamma(t)$ determined by B^{-1}, and a long-time power-law decay

$$\Gamma(t) \sim t^{-(l+3/2)} \quad (3.10)$$

for $t \rightarrow \infty$. The short-time decay of $\Gamma(t)$ is governed by the "width of the width function," i.e., by the width of the distribution of the discrete-continuum coupling strength over the continuous spectrum. The long-time decay of $\Gamma(t)$, on the other hand, is determined by the threshold onset of $\Gamma(E)$. We may anticipate that memory effects are relatively less important for typical shape resonances ($l>0$) than for s-wave sccattering ($l=0$) or for electron scattering from polar molecules, where we may have an effective $l<0$ as a consequence of the long-range dipole potential.[65,66] These qualitative trends will be illustrated for specific examples below.

B. Method of solution

An obvious, though indirect, way to obtain solutions of the time-dependent equation of motion is to calculate the time-independent wave function $\psi_{d,E}(R)$ defined by Eq. (2.21) and then transform to the time domain via

$$\psi_d(R,t)=i\int_{-\infty}^{\infty}\frac{dE}{2\pi}e^{-iEt}\psi_{d,E}(R) . \quad (3.11)$$

For the present model this indirect method can be employed very efficiently, since the projections $\langle v|\psi_{d,E}\rangle$ of the time-independent wave function on the harmonic-oscillator basis functions can be obtained by three-term recursion relations and continued fractions.[63-65] This numerical scheme is extremely efficient and stable, and allows, therefore, an essentially unlimited number of these elements to be calculated for an essentially unlimited range of energies. For more realistic problems, however, in particular, those involving open rearrangement and break-up channels, the computation of $\psi_{d,E}(R)$ over a very wide range of energies would be technically very tedious and would require an enormous amount of computing time.

We therefore found it more attractive, in particular with regard to future applications of the theory to more realistic models, to explore the possibility of a direct solution of Eq. (2.12) in the time domain. As pointed out by McCurdy and Turner,[31] a possible advantage of such a direct method of solution lies in the generally very short lifetime of resonance states, which should allow us to confine the propagation of $\psi_d(t)$ to a fairly short time interval.

As a first step in this direction we have developed a simple and efficient procedure to solve Eq. (2.12) directly in time for the class of models introduced above. First, the wave packet $\psi_d(Q,t)$ is expanded in terms of harmonic-oscillator basis functions (eigenfunctions of $\tilde{H}_0$)

$$\psi_d(Q,t)=\sum_{v=0}^{N}C_v(t)\chi_v(Q) . \quad (3.12)$$

This expansion converts Eq. (2.12) into a system of coupled integro-differential equations in time only

$$i\frac{dC_v(t)}{dt}=\sum_{v'=0}^{N}H_{vv'}^{(d)}C_{v'}(t)+\frac{1}{i}\int_0^t dt' F_{vv}(t-t')C_v(t') , \quad (3.13)$$

where

$$H_{vv'}^{(d)}=\langle v|\tilde{H}_d|v'\rangle , \quad (3.14)$$

and $F_{vv}(t)$ is given by Eq. (3.9). For the shifted-harmonic-oscillator model, the matrix $H_{vv'}^{(d)}$ is tridiagonal in v,v'

$$H_{vv}^{(d)}=(v+\tfrac{1}{2})\omega+\varepsilon , \quad (3.14a)$$

$$H_{v,v-1}^{(d)}=(v/2)^{1/2}\kappa . \quad (3.14b)$$

We next expand the coefficients $C_v(t)$ and the integral kernels $F_{vv}(t)$ in terms of Laguerre polynomials

$$C_v(t)=\sum_{\beta=0}^{K}C_v^{\beta}L_\beta(\gamma t)e^{-\gamma t/2} , \quad (3.15a)$$

$$F_{vv}(t)=\sum_{\alpha=0}^{K}F_{vv}^{(\alpha)}L_\alpha(\gamma t)e^{-\gamma t/2} . \quad (3.15b)$$

The scaling parameter γ is arbitrary and can be chosen to optimize the convergence of these expansions. For the present applications the choice $\gamma=\omega$ was found to be appropriate. The expansions (3.15) are motivated by the fact that the convolution integral of two Laguerre polynomials is again a linear combination of Laguerre polynomials.[71] Expansions in terms of Laguerre polynomials have been employed previously to solve integro-differential equations.[72,73]

The expansion coefficients $F_{vv}^{(\alpha)}$ of the integral kernels are straightforwardly calculated as

$$\begin{aligned} F_{vv}^{(\alpha)} &= \int_0^\infty d(\gamma t) F_{vv}(t) L_\alpha(\gamma t) e^{-\gamma t/2} \\ &= \frac{(-1)^\alpha A \gamma e^{X_v}}{(2\pi i)\alpha!} \sum_{j=0}^{\alpha} \begin{bmatrix} \alpha \\ j \end{bmatrix} X_v^{\alpha-j} \Gamma(1+j+l+\tfrac{1}{2}) \sum_{p=0}^{\alpha} (-1)^p \begin{bmatrix} \alpha \\ p \end{bmatrix} X_v^{l+1/2-j-p} \Gamma(-l-\tfrac{1}{2}-j+p, X_v) , \end{aligned} \tag{3.16a}$$

where

$$X_v = [(v+\tfrac{1}{2})\omega - i\gamma/2]/B \tag{3.16b}$$

and $\Gamma(a,x)$ denotes the incomplete gamma function.[71] The direct computation of $F_{vv}^{(\alpha)}$ (terms up to $\alpha=120$ will be needed in some cases) is very time consuming and, moreover, numerically unstable. A more practical scheme is the computation of $F_{vv}^{(\alpha)}$ by upward recursion in α. We define the auxiliary integral

$$M_v^{(\alpha)} = \int_0^\infty \frac{dE}{2\pi} A(E/B)^{l+1/2} e^{-E/B} (Y_v + iE/\gamma) \int_0^\infty d(\gamma t) L_\alpha(\gamma t) e^{-i\gamma(Y_v+iE/\gamma)t} , \tag{3.17}$$

where $Y_v = iBX_v/\gamma = i(v+\frac{1}{2})\omega/\gamma + \frac{1}{2}$. Using these definitions and properties of the Laguerre polynomials, we find the four-term recursion relation

$$\begin{aligned} (\alpha+1) Y_v M_v^{(\alpha+2)} &= [1+\tfrac{1}{2}-\alpha+(3\alpha+2-i\gamma/B)Y_v] M_v^{(\alpha+1)} \\ &\quad + [-l-\tfrac{1}{2}+2\alpha-(3\alpha+1-i\gamma/B)Y_v - i\gamma/B] M_v^{(\alpha)} + \alpha(Y_v-1) M_v^{(\alpha-1)} . \end{aligned} \tag{3.18}$$

To start the recursion, $M_v^{(0)}$ and $M_v^{(1)}$ are computed from analytic expressions analogous to Eq. (3.16), which follow from the definition (3.17). The desired coefficients are finally obtained from

$$F_{vv}^{(\alpha)} = M_v^{(\alpha)} - M_v^{(\alpha+1)} . \tag{3.19}$$

Inserting the expansions (3.15a) and (3.15b) into the coupled equations (3.13) and comparing coefficients, we obtain the following set of linear algebraic equations for the C_v^β:

$$\begin{aligned} i\gamma[\beta C_v^\beta - (\beta+1) C_v^{\beta+1}] &= \left[\varepsilon + (v+\tfrac{1}{2})\omega + \frac{i\gamma}{2}\right] [-\beta C_v^{\beta-1} + (2\beta+1) C_v^\beta - (\beta+1) C_v^{\beta+1}] \\ &\quad + \sum_{v'} H_{vv'}^{(d)} [-\beta C_{v'}^{\beta-1} + (2\beta+1) C_{v'}^\beta - (\beta+1) C_{v'}^{\beta+1}] \\ &\quad + \frac{1}{i\gamma} \sum_\alpha F_{vv}^{(\alpha)} [\beta C_v^{\beta-\alpha-2} - (3\beta+1) C_v^{\beta-\alpha-1} + (3\beta+2) C_v^{\beta-\alpha} - (\beta+1) C_v^{\beta-\alpha+1}] . \end{aligned} \tag{3.20}$$

This set of equations is to be complemented by the initial condition (3.6) which takes, for a target molecule in its vibrational ground level, the form

$$\sum_\beta C_v^\beta = \delta_{v,0}, \quad v=0,1,2,\ldots . \tag{3.21}$$

Taking account of the tridiagonality of $H_{vv'}^{(d)}$, Eq. (3.20) can be compactly written as

$$\underline{X}_v \underline{C}_{v-1} + \underline{Y}_v \underline{C}_v + \underline{Z}_v \underline{C}_{v+1} = \underline{0}, \quad v=0,1,2,\ldots \tag{3.22}$$

where $\underline{C}_v$ is the vector with elements C_v^β, $\beta=0,1,2,\ldots,K$. The $\underline{X}_v, \underline{Y}_v, \underline{Z}_v$ are rectangular matrices with K rows and $K+1$ columns defined by Eq. (3.20). The initial condition (3.21) can now be incorporated in compact form as follows. We augment the matrices $\underline{X}_v, \underline{Y}_v, \underline{Z}_v$ by one additional bottom row to obtain square $(K+1)\times(K+1)$ matrices $\underline{X}_v', \underline{Y}_v', \underline{Z}_v'$. For $\underline{Y}_v'$, the elements in the last row are unity, for $\underline{X}_v'$ and $\underline{Z}_v'$ they are zero. We then have

$$\underline{Y}_0' \underline{C}_0 + \underline{Z}_0' \underline{C}_1 = \underline{a} , \tag{3.23a}$$

$$\underline{X}_v' \underline{C}_{v-1} + \underline{Y}_v' \underline{C}_v + \underline{Z}_v' \underline{C}_{v+1} = \underline{0}, \quad v=0,1,2,\ldots \tag{3.23b}$$

where $\underline{a}$ is the $(K+1)$-dimensional vector with elements

$$a^\beta = \delta_{\beta,K+1}, \quad \beta=0,1,2,\ldots,K+1 . \tag{3.23c}$$

Equations (3.23) can equivalently be written as an inhomogeneous system of linear equations in supermatrix form

$$\begin{pmatrix} \underline{Y}_0' & \underline{Z}_0' & & & \\ \underline{X}_1' & \underline{Y}_1' & \underline{Z}_1' & & \\ & \underline{X}_2' & \underline{Y}_2' & \underline{Z}_2' & \\ & & \underline{X}_3' & \underline{Y}_3' & \underline{Z}_3' \\ & & & & \ddots \end{pmatrix} \begin{pmatrix} \underline{C}_0 \\ \underline{C}_1 \\ \underline{C}_2 \\ \underline{C}_3 \\ \vdots \end{pmatrix} = \begin{pmatrix} \underline{a} \\ \underline{0} \\ \underline{0} \\ \underline{0} \\ \vdots \end{pmatrix} . \tag{3.24}$$

In a typical application (see below) we have to include about 50 oscillator functions in the expansion (3.12) and about 100 Laguerre polynomials in the expansions (3.15a) and (3.15b), resulting in a dimension of 5000 of the matrix of coefficients in Eq. (3.24). To solve this large set of equations efficiently, we make use of the tridiagonal supermatrix structure, which allows us to construct the inverse as a matrix continued fraction.

To derive the continued fraction, we put $\underline{C}_{M+1}=0$ for some sufficiently large M $(M>N)$ to obtain

$$\underline{C}_M = -(\underline{Y}_M')^{-1}\underline{X}_M'\underline{C}_{M-1} .$$

Using, repeatedly, the recursion relations (3.23b), we obtain an expression for $\underline{C}_{M-v}$ in terms of $\underline{C}_{M-v-1}$

$$\underline{C}_{M-v} = -\left[\underline{Y}_{M-v}' - \underline{Z}_{M-v}'(\underline{Y}_{M-v+1}' - \underline{Z}_{M-v+1}'(\cdots)^{-1}\underline{X}_{M-v+2}')^{-1}\underline{X}_{M-v+1}'\right]^{-1}\underline{X}_{M-v}'\underline{C}_{M-v-1} .$$

Putting $v=M-1$ and using Eq. (3.23a), we obtain $\underline{C}_0$ as a matrix continued fraction

$$\underline{C}_0 = \left[\underline{Y}_0' - \underline{Z}_0'\left[\underline{Y}_1' - \underline{Z}_1'\left[\cdots\right]^{-1}\underline{X}_2'\right]^{-1}\underline{X}_1'\right]^{-1}\underline{a} . \tag{3.25}$$

The $\underline{C}_v$ with $v>0$ are finally calculated from Eq. (3.23b) by forward recursion.

This scheme, together with the recursive calculation of the matrix elements $F_{vv'}^{(\alpha)}$, defines a completely recursive and, therefore, extremely efficient numerical method to solve the space-time integro-differential equation (2.12). All recursions have been found to be numerically stable. Once the expansion coefficients C_v^β are obtained, the wave packet $\psi_d(Q,t)$ is calculated from Eqs. (3.12) and (3.15a) using recursive computation of the Laguerre and Hermite polynomials.

Since the Laplace transform of a product of Laguerre polynomials and exponentials can be evaluated analytically, we can express the $0\rightarrow v$ T-matrix element explicitly in terms of the coefficients C_v^β

$$T_{v0}(E) = -iV_{d\mathbf{k}_j}^* V_{d\mathbf{k}_i} \sum_{\beta=0}^{K} C_v^\beta \frac{(-iE-\gamma/2)^\beta}{(-iE+\gamma/2)^{\beta+1}} . \tag{3.26}$$

This formula provides interesting insight into the nature of the solution obtained by the present approximation scheme. The analytic continuation of $T_{v0}(E)$ into the complex energy plane obviously exhibits poles of order $1,2,3,\ldots,K+1$ at the single energy $E=-i\gamma/2$. This crazy pole structure is a consequence of the expansion (3.15a), which yields an exponentially decaying wave function for $t\rightarrow\infty$ for any finite K, while the decay of the exact wave function is necessarily nonexponential for $t\rightarrow\infty$ (see, e.g., Ref. 74). Nevertheless, as will be demonstrated below, $T_{v0}(E)$ of Eq. (3.26) yields the correct result for *real* energy E to any desired accuracy if K is chosen sufficiently large.

The solution of the equation of motion in the LCP approximation, Eq. (2.29), is trivial and need not be described in detail. Expanding $\psi_d(Q,t)$ in the harmonic-oscillator basis set, we obtain a system of coupled first-order differential equations with constant coefficients. The solution is immediately obtained by diagonalizing the (complex-symmetric) matrix of coefficients.

IV. ILLUSTRATIVE APPLICATIONS

A. Model of the $^2\Pi_g$ shape resonance in $e+N_2$ scattering

The $^2\Pi_g$ d-wave shape resonance in $e+N_2$ scattering is by far the most thoroughly studied resonance phenomenon in the field of electron-molecule scattering, both experimentally[75–77] and theoretically.[3,10,12,13,31,35,41,61,78–81] The now well-known "boomerang" model has been developed for this system in order to explain the intriguing vibrational interference structure of the $0\rightarrow v$ excitation cross sections.[57] The time-dependent description of nuclear motion in the $^2\Pi_g$ shape resonance of $e+N_2$ has already been discussed by McCurdy and Turner within the LCP approximation.[31] We have chosen this well-known system in order to illustrate the concepts and to check the performance of our numerical techniques.

The model described in Sec. III, characterized by harmonic potentials and the $\Gamma(E)$ approximation, has been applied earlier to this resonance and shown to provide a surprisingly reliable qualitative description of the $0\rightarrow v$ excitation functions for many vibrational channels.[61] The model has correctly predicted the qualitative behavior of the deeply inelastic excitation functions which have been measured only recently (up to $v=17$).[77] It may thus be stated that the model, despite its obvious idealizations, provides an authentic description of the basic features of the dynamics of N_2^- in the $^2\Pi_g$ state.

The present model of the $^2\Pi_g$ shape resonance (model I) is the same as considered previously,[59,61] except for a slightly different (more realistic) parametrization of the width function. The parameters $A,B,l,\omega,\varepsilon,\kappa$ specifying the model according to Eqs. (3.2) and (3.4) are collected in Table I. Figure 1 shows the width function $\Gamma(E)$ and the corresponding level-shift function $\Delta(E)$. The former represents the distribution of the discrete-continuum coupling strength over the continuous spectrum and is available from *ab initio* calculations.[33,38] Figure 2(a) shows the model potential-energy curves of N_2 (solid line) and the real part of the LCP energy of N_2^- (dashed line) defined in Eq. (2.24). Figure 2(b) shows the corresponding imaginary part, that is, the local width function $\Gamma(Q)$ of this resonance state. It is seen that the *local* width is strongly Q dependent, which is a consequence of the Q dependence of the discrete-state energy $V_d(Q)-V_0(Q)$ and the energy dependence of $\Gamma(E)$ [see Eqs. (2.24)–(2.26)]. In Fig. 3 we show the calculated vibrational excitation cross sections for the channels $0\rightarrow 1$, $0\rightarrow 2$, and $0\rightarrow 9$ as representative examples. They exhibit the well-known boomerang-type vibrational interference structure[78–80] and compare well with the experiment,[75–77] even with respect to finer details of the peak shapes.

The technical details of the present numerical calculations, as outlined in Sec. III B, can be summarized as follows. First of all, it was found to be preferable for this example to modify the expansion (3.15a) to read

$$C_v(t)=e^{-i\varepsilon t}\sum_{\beta=0}^{K}\tilde{C}_v^{\beta}L_\beta(\gamma t)e^{-\gamma t/2}\ , \tag{4.1}$$

that is, we extract the rapidly oscillating factor $\exp(-i\varepsilon t)$ before expanding in terms of Laguerre polynomials. The expansion (4.1) was truncated at $K=100$, i.e., 101 Laguerre polynomials are included. The matrix continued fraction (3.25), which involves matrices $\underline{X}_v', \underline{Y}_v'\underline{Z}_v'$ with dimension 101, has been truncated after 80 steps. The coefficient vectors $\underline{C}_v$ have been calculated up to $v=40$ by the three-term recursion (3.23b). This implies that the wave packet $\psi_d(Q,t)$ is expanded in terms of the lowest 41 oscillator functions according to Eq. (3.12). With these truncations complete convergence has been achieved up to at least ten vibrational periods. The numerical results were checked for consistency and accuracy by comparing the T-matrix elements calculated from Eq. (3.26) with the corresponding elements obtained by the direct solution of the Lippmann-Schwinger equation via continued fractions.[63–65]

It is instructive to consider first the time-dependence of the memory kernel $F(Q,Q';t)$ for this model system. The matrix elements $F_{vv}(t)$ defined in Eqs. (3.7) and (3.9) are shown in Fig. 4 for $v=0$, 20, and 40. The solid line and dashed line give the real and imaginary part, respectively. It is seen that the memory of the system is of the order of 1 fs and thus about an order of magnitude smaller than the vibrational period $T=2\pi/\omega=13.5$ fs. The shortness of the memory is a consequence of the d-wave character of the resonance and the relatively large value of the cutoff parameter B. We may anticipate from inspection of Fig. 4 that memory effects will not be of primary importance for the $^2\Pi_g$ resonance in $e+N_2$.

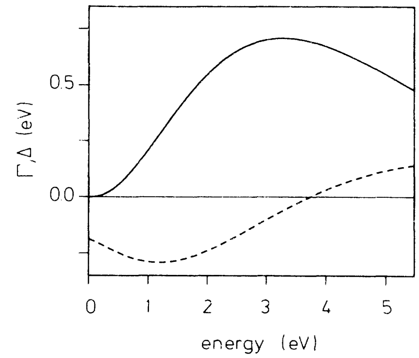

FIG. 1. Width function $\Gamma(E)$ (solid line) and level shift $\Delta(E)$ (dashed line) for model I, representing the $^2\Pi_g$ d-wave shape resonance in $e+N_2$.

Figure 5 shows, for illustrative purposes, expansion coefficients $C_v(t)$ defined in Eq. (3.12) for $v=0$, 5 and 10. The $C_v(t)$ exhibit a rapid oscillation with a frequency roughly given by the (vertical) discrete-state energy ε as well as recurrences with approximately the vibrational period T. The coefficient $C_0(t)$ represents the autocorrelation function, that is, the overlap of the time-dependent wave packet $\psi_d(t)$ with the initial packet $\psi_d(0)$.

The absolute square of the wave packet $\psi_d(Q,t)$, constructed from these coefficients according to Eq. (3.12), is shown in Fig. 6 in time steps of 1.5 fs up to 16.5 fs. Owing to the very rapid decay of the wave packet, it is necessary to magnify $|\psi_d|^2$ at later times as indicated in the figure. The wave packet at $t=0$ is a Gaussian, given by the ground-state wave function of the harmonic oscillator $\tilde{H}_0$. It is seen from Fig. 6 that the wave packet exhibits the expected decay and oscillatory motion. It is noteworthy that the wave packet essentially retains its Gaussian shape over the relevant range of times.

In order to catch the essentials of the wave-packet dynamics more quantitatively, it is useful to introduce the following quantities. The *decay* dynamics of the system is characterized by the survival probability of the wave packet

TABLE I. Parameters of models I, II, and III [see Eqs. (3.2) and (3.4)]. All quantities, except the integer l, are in eV.

Model	l	A	B	ω	ε	κ
I	2	0.874	1.316	0.29	2.35	−0.38
II	1	1.482	0.625	0.30	0.50	−0.25
III	0	2.085	1.470	0.17	0.88	−0.17

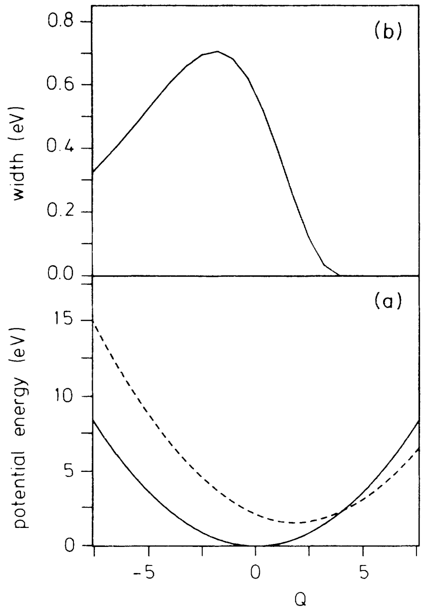

FIG. 2. Local potential-energy curves (a) and local width function $\Gamma(Q)$ (b) for model I. The potential energy of the target is given by the solid line in (a), the real part of the resonance potential energy by the dashed line.

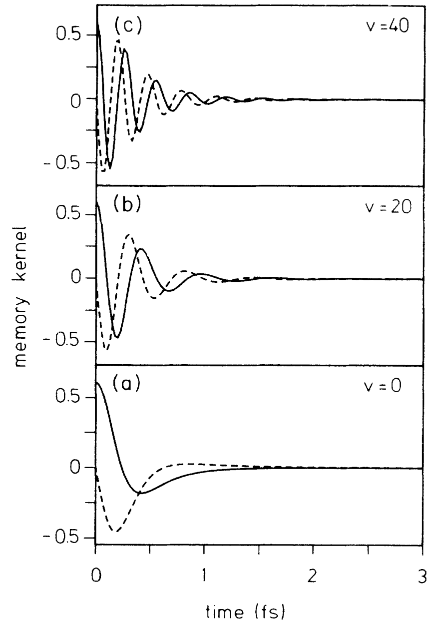

FIG. 4. Representative matrix elements $F_{vv}(t)$ of the memory kernel of model I, for $v=0$, 20, and 40. Solid and dashed lines represent real and imaginary parts, respectively.

$$S(t)=\langle\psi_d(t)|\psi_d(t)\rangle=\int dQ|\psi_d(Q,t)|^2 . \tag{4.2}$$

The vibrational dynamics of the system, on the other hand, is concisely described by the mean values of position and momentum

$$\langle Q\rangle=\langle\psi_d(t)|Q|\psi_d(t)\rangle/S(t) , \tag{4.3a}$$

$$\langle P\rangle=\langle\psi_d(t)|P|\psi_d(t)\rangle/S(t) , \tag{4.3b}$$

where $P=-id/dQ$ is the momentum operator of nuclear motion. Since, as shown in Fig. 6, the shape of the wave packet remains approximately unchanged, these three quantities contain the essential information on the dy-

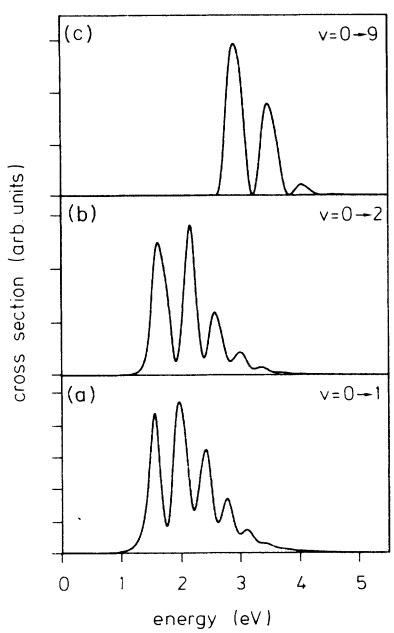

FIG. 3. Representative vibrational excitation functions for model I, exhibiting the familiar boomerang-type vibrational interference structure (Refs. 57 and 78).

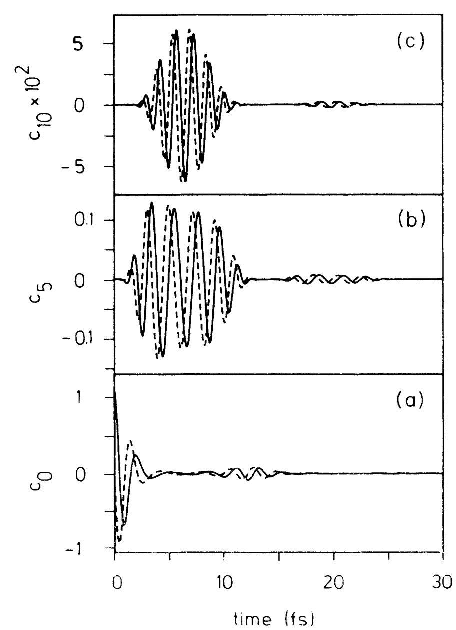

FIG. 5. Time-dependent expansion coefficients $C_v(t)$ of the wave packet of model I in terms of harmonic-oscillator basis functions, for $v=0$, 5, and 10. The solid (dashed) line represents the real (imaginary) part.

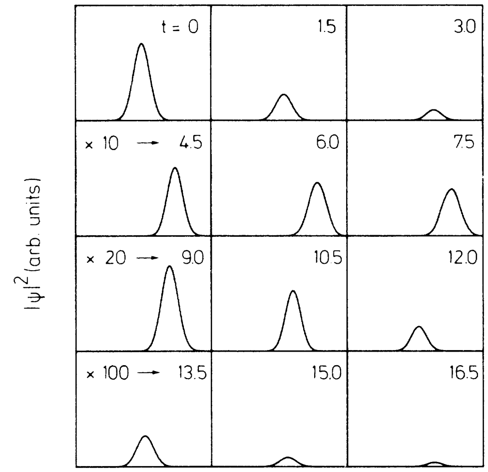

FIG. 6. Time evolution of the wave packet $\psi_d(Q,t)$ for model I, propagated with the integro-differential equation (2.12). Time is given in femtoseconds, the abscissa is from $Q=-6$ to $Q=6$ for each plot. At later times the wave packet has been magnified as indicated in the figure.

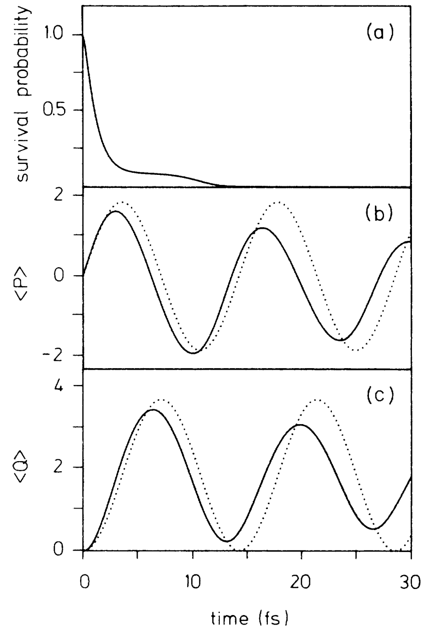

FIG. 7. Survival probability (a), mean momentum (b), and mean position (c) of the exact wave packet for model I. The dotted line in (b) and (c) represents the motion of the wave packet in the absence of decay ($\Gamma \equiv 0$).

namics of the collision complex.

Figure 7(a) displays the electronic decay of the wave packet. The survival probability exhibits a fast initial decay within the first five femtoseconds, which flattens out between 5 and 10 fs as the wave packet moves into a region of smaller (local) width. A second fast decay of the survival probability is observed as the wave packet returns into the Franck-Condon region, where the local width is large. The result in Fig. 7(a), obtained by the exact solution of the integro-differential equation (2.12), is in complete accord with the qualitative picture (boomerang model) envisaged two decades ago by Herzenberg,[57] as well as with quantitative results obtained for this system (in a more realistic model) in the LCP approximation.[31]

Figures 7(b) and 7(c) exhibit in more detail the vibrational motion of the wave packet. The dotted curves show the harmonic motion which would result in the absence of coupling to the continuum ($\Gamma=0$). We notice a slight reduction of the vibrational period compared to the $\Gamma=0$ case, which is explained by the distortion of the real part of the LCP [dashed curve in Fig. 2(a)] through the local level shift $\Delta(Q)$. We notice, moreover, a slight damping of the amplitude of the oscillatory motion which has apparently not been noted before in qualitative or quantitative discussions of the boomerang model.[31,57] This phenomenon will be discussed in more detail for model II below.

The wave packet and the quantities $S(t)$, $\langle Q \rangle$, and $\langle P \rangle$ calculated in the LCP approximation (more precisely, the semilocal approximation, see Sec. II C) for the present model are virtually indistinguishable from the exact results shown in Figs. 6 and 7 and are therefore not displayed here. This result confirms once more (see Refs. 13, 31, 41, 61, 78, and 79) the excellent quantitative accuracy of the LCP approximation for the $^2\Pi_g$ resonance in $e+N_2$.

In summary, the model for the $^2\Pi_g$ resonance in $e+N_2$ provides an excellent test for the performance of the numerical techniques which we have employed to solve the integro-differential equation (2.12). The results confirm the expected equivalence of the exact nonlocal and non-Markovian theory with the LCP approximation for this particular system. The reason for the excellent performance of the LCP approximation is the shortness of the memory as documented in Fig. 4.

B. Model of a *p*-wave resonance near threshold

Our second example (model II) is chosen such as to reveal the characteristic effects of memory and nonlocality which are to be expected for shape resonances that cross the continuum threshold as a function of the internuclear distance. We consider a *p*-wave shape resonance [$l=1$ in Eq. (3.4)]. To keep some connection with reality, in particular as far as memory effects are concerned, the parameters A and B of the width function $\Gamma(E)$ are determined from an *ab initio* calculation for the $^2\Sigma_u^+$ *p*-wave shape resonance in $e+F_2$ at the equilibrium geometry of F_2.[34] Figure 8 displays $\Gamma(E)$ and the real level-shift function $\Delta(E)$. In comparison with Fig. 1 for the $^2\Pi_g$ resonance in $e+N_2$, the width increases more rapidly with energy and also peaks at considerably lower energy. The potential parameters ε and κ in Eq. (3.2b) have been chosen such that the local potential of the resonance is crossed by the potential-energy curve of the target near the minimum of the former, as shown in Fig. 9(a). It is seen from Figs. 9(a) and 9(b) that the negative ion will explore, during its vibrational motion, both real and com-

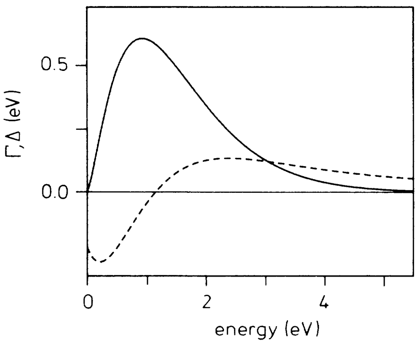

FIG. 8. Width function $\Gamma(E)$ (solid line) and level-shift function $\Delta(E)$ (dashed line) for model II, representing a p-wave shape resonance.

plex parts of the effective local potential (in contrast to the foregoing example, where the crossing of the N_2 and N_2^- potentials is outside the range of vibrational motion). The values of the parameters specifying the model are collected in Table I.

Figure 10 shows, for the purpose of illustration, the elastic and the first inelastic cross section for this model. We observe boomerang-type oscillations which are narrow close to threshold and become broader with increasing energy, thus reflecting the variation of the decay width with energy. Qualitatively similar features are observed, for example, in electron scattering from NO,[82] indicating that the present model is not physically unreasonable (see Ref. 83 for a theoretical model of the e +NO resonances).

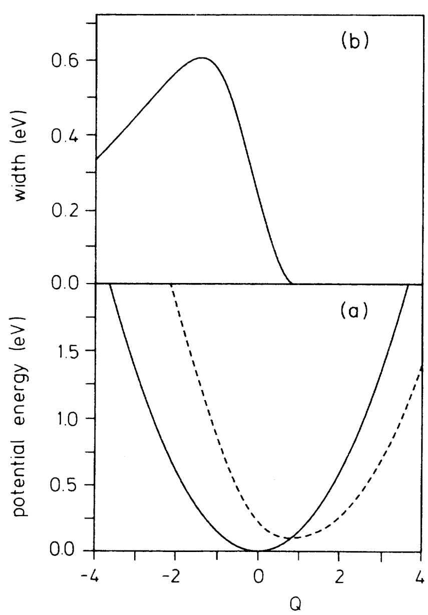

FIG. 9. Local potential-energy curves (a) and local width function $\Gamma(Q)$ (b) for model II. The solid line in (a) represents the target molecule; the dashed line the negative ion.

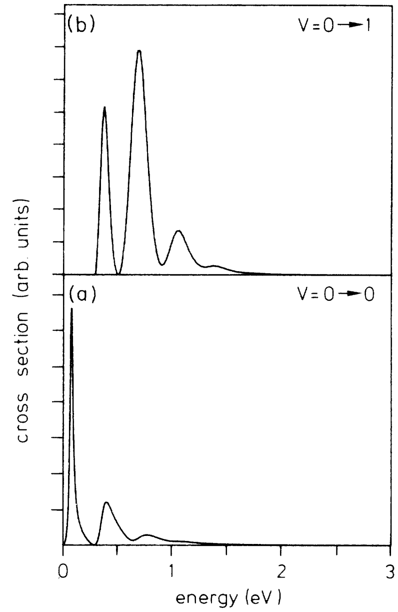

FIG. 10. Elastic and first inelastic electron-scattering cross section for model II.

Representative matrix elements of the memory kernel $F_{vv}(t)$ are shown in Fig. 11. It is seen that the memory extends now beyond 3 fs and is thus significantly longer than in the first example. This is a consequence of the fact that $\Gamma(E)$ is considerably narrower and peaked at lower energy than in the first example.

The time-dependent wave packet, representing the exact solution of the equation of motion (2.12), is depicted in Fig. 12 in time steps of 1 fs for the first 11 fs. Although nonlocal effects and memory effects will be seen to be significant in this example, we observe that the wave packet at least approximately retains its Gaussian shape (it does so also for longer times not shown in Fig. 12). This observation indicates that semiclassical approximation methods based on simple Gaussian wave-packet propagation[21–23] might be useful even beyond the LCP approximation discussed in Ref. 31.

In Fig. 13 the dynamics of the system is characterized by the survival probability, the mean position, and the mean momentum (solid curves). The corresponding quantities calculated in the LCP approximation (more precisely, the semilocal approximation) are included as dashed curves. For $\langle Q \rangle$ and $\langle P \rangle$ we show also the harmonic motion which would result in the absence of coupling to the continuum ($\Gamma \equiv 0$, dotted curves).

The survival probability $S(t)$ calculated in the LCP approximation exhibits the "staircase" behavior expected for a wave packet which moves in a potential that is partly complex and partly real (see Fig. 9). The exact survival probability, in contrast, shows clearly a nonmonotonic dependence on time. It is seen to increase while the wave packet moves on the electronically bound part of the potential energy curve of the collision complex. This implies that electrons are recaptured from the continuum by

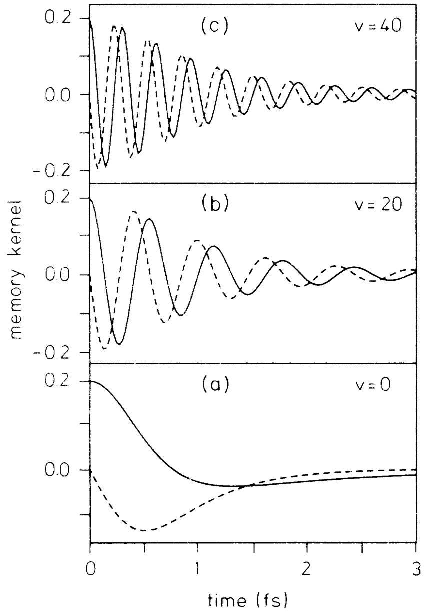

FIG. 11. Representative matrix elements $F_{vv}(t)$ of the memory kernel of model II, for $v=0$, 20, and 40. Solid and dashed lines represent real and imaginary parts, respectively.

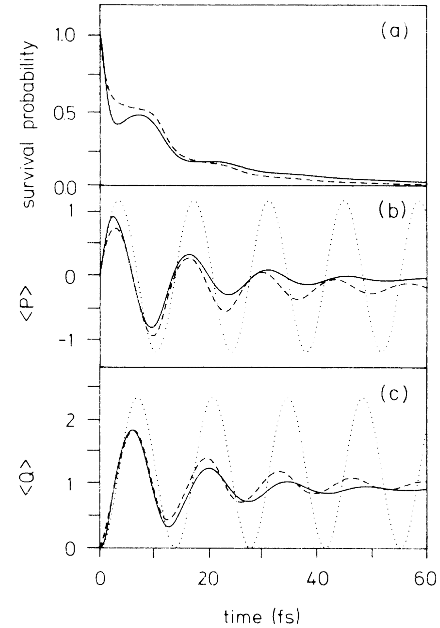

FIG. 13. Survival probabillity (a), mean momentum (b), and mean position (c) of the wave packet for model II. Solid line: exact results, Eq. (2.12). Dashed line: LCP approximation, Eq. (2.29). The dotted line in (b) and (c) represents the motion of the wave packet in the absence of decay ($\Gamma \equiv 0$).

interconversion of electronic and vibrational energy. The nonmonotonic behavior of $S(t)$ is a characteristic memory effect because it is strictly excluded in the Markovian approximation. Physically, it reflects the fact that the time scale for the disappearance of continuum electrons is not infinitely fast compared with the period of vibrational motion. At long times the exact $S(t)$ decays more slowly than the $S(t)$ calculated in the LCP approximation, which is presumably a consequence of the recapture effect in the exact theory.

A closer inspection of the wave-packet motion in Fig. 12 reveals that the amplitude of vibrational motion is noticeably smaller than expected based on the potential-energy curves in Fig. 9(a). This effect, which is in fact dramatic, is exhibited more clearly by the functions $\langle Q \rangle$ and $\langle P \rangle$ in Figs. 13(b) and 13(c). It is seen that the amplitude of vibrational motion as well as the maximum velocity decrease rapidly with time, the wave packet coming to a nearly complete standstill within about three vibrational periods. The wave-packet motion thus closely resembles that of a harmonic oscillator with friction, see, e.g., Refs. 84–86. It should be noted that the vibrational motion is damped out before the wave packet has completely decayed, in contrast to our first example, where the frictional effects are much weaker.

A qualitative explanation of the pronounced damping of the vibrational motion can be given as follows. As a consequence of the threshold law, $\Gamma(E) \sim E^{l+1/2}$, shape resonances near threshold decay preferentially via the emission of relatively fast electrons. The recapture process, on the other hand, should be more efficient for low-energy electrons, since electrons with higher energy disappear quickly. As a consequence of both effects the total energy of the ensemble of negative ions described by the wave packet $\psi_d(Q,t)$ decays faster than the population, manifesting itself in a damping of the vibrational motion. An alternative interpretation of the damping of vibrational motion could be in terms of a dephasing process, that is, loss of coherence of the initially prepared wave packet. However, the fact that we do not observe any significant broadening of the wave packet with time does not support this interpretation.

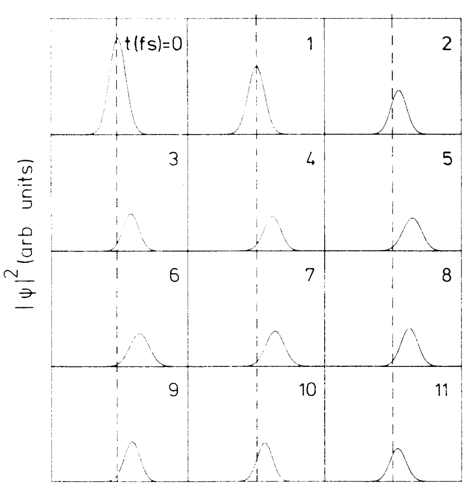

FIG. 12. Time evolution of the wave packet $\psi_d(Q,t)$ for model II, propagated with the integro-differential equation (2.12). Time is given in femtoseconds; the abscissa is from $Q=-6$ to $Q=6$ for each plot.

It is seen from Fig. 13 that the LCP approximation, though not quantitatively accurate, reproduces surprisingly well the damped oscillatory motion of the wave packet. At long times, the damping in the LCP approximation is noticeably weaker than in the exact calculation. This is presumably a consequence of the absence of recapture processes in the Markovian approximation. In the LCP approximation the damping of the vibrational motion must be ascribed to a (negative) imaginary part of the effective vibrational frequency resulting from the (positive) second derivative of the local width function $\Gamma(Q)$ in the relevant range of Q. The damping would be absent in the LCP approximation if $\Gamma(Q)$ were approximated by a linear function of Q as in Ref. 10.

In summary, this example of a p-wave shape resonance near threshold conspicuously exhibits memory effects in the decay dynamics and frictional effects in the vibrational dynamics. The results demonstrate that the phenomenology of wave-packet dynamics in short-lived negative ions is vastly richer than the wave-packet dynamics on "standard" (that is real, local, and Markovian) potential-energy curves.

C. Model of s-wave scattering and virtual-state effects

It has been shown that the class of models considered here naturally describes bound-state and virtual-state threshold effects in s-wave scattering if the width function $\Gamma(E)$ possesses the appropriate threshold behavior [$l=0$ in Eq. (3.4)].[66,68] If the threshold exponent $\alpha=l+\frac{1}{2}$ is taken to be smaller than $\frac{1}{2}$, the model also accounts for dipole-induced threshold effects in electron scattering from polar molecules.[65,66]

In our third example (model III), we briefly address the time-dependent description of virtual-state and bound-state threshold effects in s-wave scattering. A detailed analysis of the rather complex dynamics of s-wave electron-molecule collision complexes is beyond the scope of this paper and is deferred to a future publication.

The model is the same as employed previously[68] for a quantitative analysis of the virtual-state effect in low-energy electron-CO_2 scattering.[87-89] In order to render the vibrational dynamics of the collision complex more conspicuous, we have chosen here a larger electron-vibrational coupling constant κ (the electron-vibrational coupling is rather weak in $e+CO_2$). The parameters of the model are included in Table I.

A characteristic phenomenon in s-wave scattering are Wigner cusps in the cross sections at the opening of inelastic channels.[90] These Wigner cusps show up distinctively in the present model, as demonstrated by Fig. 14, where the elastic ($v=0\rightarrow0$) cross section is shown. Wigner cusps are clearly seen at the $v=1$, 2, and 3 thresholds. The large enhancement of the elastic cross section towards $E=0$ is the consequence of a virtual-state pole of the fixed-nuclei S-matrix close to the origin (see Ref. 68 for details).

The solid line in Fig. 14 gives the result of the time-dependent calculation, the T-matrix element being calculated from Eq. (3.26) with $K=120$ [that is, 121 Laguerre polynomials have been included in the expansion of the coefficients $C_v(t)$]. The dotted line (hardly distinguishable) represents the result of a direct time-independent calculation via continued fractions which is numerically exact. The inset in Fig. 14 shows both cross sections vertically displaced in the region of the $v=1$ and $v=2$ thresholds. The remarkable result is that the Laguerre expansion method, being a *short-time* approximation scheme, is able to reproduce nearly quantitatively the threshold cusps, which reflect the behavior of the wave function at *long* times [$E\rightarrow0$ corresponds to $t\rightarrow\infty$ according to Eqs. (2.20) and (3.11)]. This result underlines the remarks made in Sec. III B about the analytic structure of the T-matrix element $T_{v'v}$ of Eq. (3.26). It indicates, more generally, the possibility of short-time approximations for the dynamics of electron-molecule collision complexes even if threshold effects are relevant.

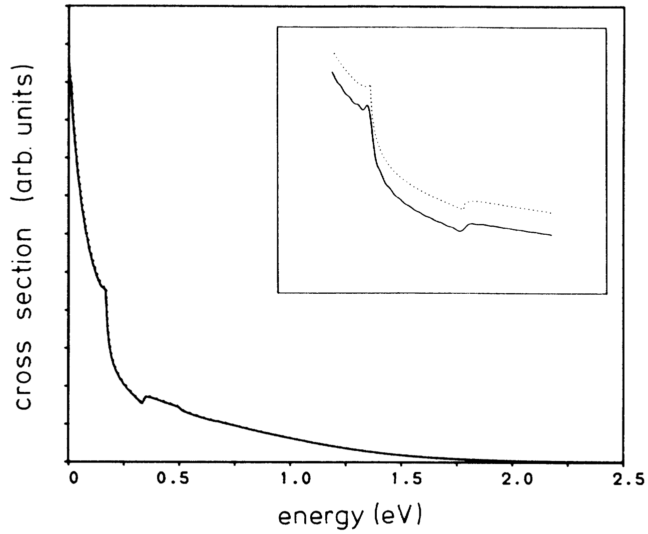

FIG. 14. Elastic ($v=0\rightarrow0$) electron-scattering cross section for model III, representing virtual-state threshold effects in s-wave scattering. Solid line: result obtained by the Laguerre expansion method with $K=120$. Dotted line: numerically exact result. Inset shows both cross sections vertically displaced in the region of the $v=1$ and $v=2$ thresholds.

Figure 15 displays in condensed form the decay dynamics and the vibrational dynamics of the s-wave model system in the exact description. Since the LCP approximation, though defined in principle,[61,66] is not a particularly useful concept for the description of resonance and threshold effects in s-wave scattering, it will not be considered here. The survival probability $S(t)$ exhibits an extremely fast initial decay (corresponding to a barrierless s-wave resonance which initially captures the electron) followed by a very slow and clearly nonmonotonic decay. In contrast to the foregoing p-wave example, where memory effects were mainly apparent at short times, we now observe memory effects (nonmonotonic population decay) mainly at longer times. They are a consequence of the slow ($t^{-3/2}$) long-time decay of the memory kernel for s-wave scattering. The small but long-lived population of negative ions represented by the long-time tail of $S(t)$ is responsible for the enhancement of the elastic cross section for $E \to 0$ and the virtual-state-induced threshold peaks in the inelastic channels.

The mean momentum and position of the wave packet, $\langle P \rangle$ and $\langle Q \rangle$, show a distinct anomaly at about 3 fs, which corresponds to the transition from the fast decay to the slow decay of $S(t)$. It reflects the nonadiabatic switchover of the wave packet from the initially populated extremely short-lived s-wave resonance to the virtual- or bound-state electronic potential-energy curve, on which it decays more slowly via nonadiabatic coupling to the continuum (see Ref. 66 for a detailed discussion of the fixed-nuclei potential-energy curves of resonances, virtual states, and bound states near the continuum threshold). During this switchover the shape of the wave packet becomes severely distorted. At later times, near 17 and 42 fs, where $\langle Q \rangle$ becomes negative, the wave packet even splits temporarily into two components. It is obvious from Fig. 15(c) that beyond ~ 4 fs the wave packet oscillates approximately about the equilibrium geometry of the *target* molecule ($Q=0$) rather than about the equilibrium geometry $\delta Q = -\kappa/\omega$ of the discrete state. This demonstrates that *threshold* effects are determining the dynamics of the collision complex after an initial time interval of only 4 fs. The absence of damping of vibrational motion seen in Figs. 15(b) and 15(c) is in accord with the qualitative explanation of the damping mechanism given above; because of the rapid $E^{1/2}$ onset of $\Gamma(E)$, there is no preference for the emission of fast electrons in s-wave scattering.

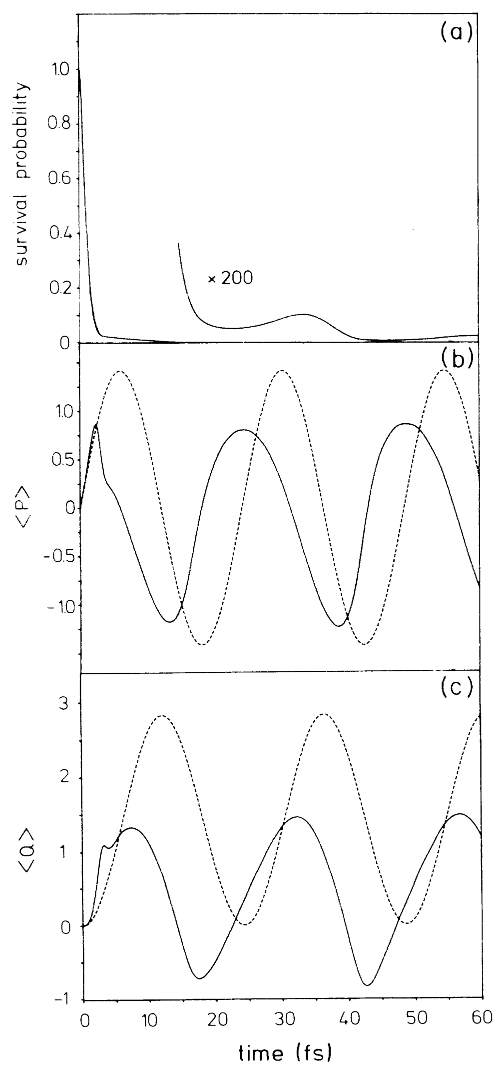

FIG. 15. Survival probability (a), mean momentum (b), and mean position (c) of the wave packet for model III. The dashed line in (b) and (c) represents the motion of the wave packet in the absence of decay ($\Gamma \equiv 0$).

In summary, the wave-packet dynamics of s-wave collision complexes is considerably more involved than the dynamics of shape resonances. Strong distortions and even splittings of the time-dependent wave packet are to be expected. We have demonstrated that our short-time approximation method based on the Laguerre expansion is remarkably successful in reproducing the multichannel Wigner-cusp structure of the cross sections.

V. CONCLUSIONS

We have outlined the time-dependent description of the electronic and nuclear dynamics of electron-molecule collision complexes within the framework of the projection-operator formalism. It has been shown that the equation of motion, which describes both electronic decay as well as vibrational and/or dissociative motion, contains effective-potential terms that are nonlocal as well as non-Markovian, i.e., account for memory effects. The relevance of the time-dependent wave packet $\psi_d(R,t)$ with the appropriate initial condition lies in the fact that it carries the complete information on the resonant scattering amplitudes for all final channels.

While non-Markovian equations of motion are well known in many areas of physics, the situation in electron-molecule collision complexes appears to be unique for two reasons, namely, (i) the non-Markovian effects can be pronounced and even dominant, and (ii) the memory kernel can be accurately calculated from first principles. While the spontaneous radiative decay of atoms (and molecules) is a non-Markovian process in principle,[49–52] the memory effects are usually minute and hardly experimentally detectable. In the field of nonequilibrium statistical mechanics, memory effects can be important, but the memory kernels are, in general, not calculable, and *ad hoc* assumptions about their properties are necessary. For electron collision complexes with simple molecules, on the other hand, the memory kernel is accurately calculable and, moreover, a large set of accurate experimental data is often available. Electron-molecule scattering thus provides the opportunity for the theoretical analysis and experimental testing of the properties of strongly non-Markovian dynamical processes.

In the present work we have set out to study basic properties of the time-dependent dynamics of electron-molecule collision complexes by the exact (numerical) solution of the nonlocal and non-Markovian equation of motion for simple models. We have developed, for this purpose, an efficient numerical scheme to solve the space-time integro-differential equation, making use of simplifying features of the model. An unambiguous identification of nonlocal and non-Markovian effects is obtained by comparison with the LCP approximation for the same model. The concepts and the performance of the numerical methods have been illustrated for a model of the $^2\Pi_g$ d-wave shape resonance in $e+N_2$, where the well-known features of the boomerang model[31,57] are reproduced.

Novel qualitative phenomena have been revealed for a model of a p-wave shape resonance near threshold. Memory effects are manifested by the nonmonotonic electronic decay, and pronounced frictional effects dominate the vibrational motion. It appears from these results that the coupling of an electronic state to an electronic continuum has a similar effect on the vibrational motion as the coupling of an oscillator to a heat bath.[84,85] Frictional effects can thus be of importance even in microscopic quantum systems with only few degrees of freedom (the smallest system to which the present considerations directly apply is $e+H_2$ in the $^2\Sigma_u^+$ symmetry). It may be expected that frictional effects are generally present in dissociative electron attachment via shape resonances.

We have also briefly considered some aspects of wave-packet propagation for s-wave collision complexes where virtual-state- or bound-state-induced threshold effects are important. It has been shown that multichannel Wigner-cusp structures can be recovered from the time-dependent solution even with short-time approximation methods. The example demonstrates that the non-Markovian dynamics of collision complexes in the presence of strong threshold effects can be very complicated, and that strong distortions and splittings of the wave packet are to be expected.

In summary, the motivation for this study has been the quest for deeper physical insight into the exact dynamics of electron-molecule collision complexes and the limitations of the LCP model. In future work we plan to obtain exact solutions for the wave-packet dynamics of more realistic models, in particular, those which account for dissociative attachment, in order to shed light on the details of the competition between electronic decay and dissociative motion in such systems.

ACKNOWLEDGMENTS

This work has been supported by the Deutsche Forschungsgemeinschaft and the Fonds der chemischen Industrie. The computations have been performed at the Leibniz Rechenzentrum der Bayerischen Akademie der Wissenschaften.

---

[1] *Electron-Molecule Collisions,* edited by I. Shimamura and K. Takayanagi (Plenum, New York, 1984).

[2] *Electron-Molecule Interactions and their Applications,* edited by L. G. Christophorou (Academic, New York, 1984), Vol. 1.

[3] N. Chandra and A. Temkin, Phys. Rev. A **13**, 188 (1976).

[4] B. I. Schneider, Phys. Rev. A **14**, 1923 (1976).

[5] H. Feshbach, Ann. Phys. (N.Y.) **19**, 287 (1962).

[6] E. P. Wigner and L. Eisenbud, Phys. Rev. **72**, 29 (1947).

[7] T. F. O'Malley, Phys. Rev. **150**, 14 (1966).

[8] J. N. Bardsley, J. Phys. B. **1**, 349 (1968); **1**, 365 (1968).

[9] F. Fiquet-Fayard, J. Phys. B **8**, 2880 (1975).

[10] W. Domcke and L. S. Cederbaum, Phys. Rev. A **16**, 1465 (1977).

[11] B. I. Schneider, M. Le Dourneuf, and P. G. Burke, J. Phys. B **12**, L365 (1979).

[12] B. I. Schneider, M. Le Dourneuf, and Vo Ky Lan, Phys. Rev. Lett. **43**, 1926 (1979).

[13] A. U. Hazi, T. N. Rescigno, and M. Kurilla, Phys. Rev. A **23**, 1089 (1981).

[14] P. G. Burke and C. J. Noble, Comments At. Mol. Phys. **18**, 181 (1986).

[15] W. Domcke, C. Mündel, and L. S. Cederbaum, Comments At. Mol. Phys. **20**, 293 (1987).

[16] F. T. Smith, Phys. Rev. **179**, 111 (1969).

[17] T. F. O'Malley, Adv. At. Mol. Phys. **7**, 223 (1971).

[18] R. J. Bieniek, Phys. Rev. A **18**, 392 (1978).

[19] J. M. Wadehra, in *Nonequilibrium Vibrational Kinetics,* Vol. 39 of *Topics of Current Physics,* edited by M. Capitelli (Springer, Berlin, 1986), p. 191.

[20] E. A. McCullough, Jr. and R. E. Wyatt, J. Chem. Phys. **54**, 3578 (1971).

[21] E. J. Heller, J. Chem. Phys. **62**, 1544 (1975).

[22] E. J. Heller, J. Chem. Phys. **64**, 63 (1976).

[23] E. J. Heller, J. Chem. Phys. **68**, 3891 (1978).

[24] K. C. Kulander, J. Chem. Phys. **69**, 5064 (1978).

[25] M. D. Feit and J. A. Fleck, Jr., J. Chem. Phys. **78**, 301 (1983).

[26] R. Kosloff, J. Phys. Chem. **92**, 2087 (1988).

[27] J. Alvarellos and H. Metiu, J. Chem. Phys. **88**, 4957 (1988).

[28] J. Kucar, H.-D. Meyer, and L. S. Cederbaum, Chem. Phys. Lett. **140**, 525 (1987).

[29] P. Pechukas, Phys. Rev. **181**, 166,174 (1969).

[30] W. H. Miller, Adv. Chem. Phys. **25**, 69 (1974).

[31] C. W. McCurdy and J. L. Turner, J. Chem. Phys. **78**, 6773 (1983).

[32] W. Domcke and H. Estrada, J. Phys. B **21**, L205 (1988).

[33] A. U. Hazi, in *Electron-Atom and Electron-Molecule Collisions,* edited by J. Hinze (Plenum, New York, 1983), p. 103.

[34] A. U. Hazi, A. E. Orel, and T. N. Rescigno, Phys. Rev. Lett. **46**, 918 (1981).

[35] B. M. Nestmann and S. D. Peyerimhoff, J. Phys. B **18**, 4309 (1985).

[36] N. Komiha, J. P. Daudey, and J. P. Malrieu, J. Phys. B **20**, 4375 (1987).

[37] M. Rajzmann, F. Spiegelmann, and J. P. Malrieu, J. Chem. Phys. **89**, 433 (1988).

[38] M. Berman and W. Domcke, Phys. Rev. A **29**, 2485 (1984).

[39] M. Berman, C. Mündel, and W. Domcke, Phys. Rev. A **31**, 641 (1985).

[40] V. Krumbach and B. M. Nestmann (private communication).

[41] M. Berman, H. Estrada, L. S. Cederbaum, and W. Domcke, Phys. Rev. A **28**, 1363 (1983).

[42] C. Mündel, M. Berman, and W. Domcke, Phys. Rev. A **32**, 181 (1985).

[43] M. S. Child, *Molecular Collision Theory* (Academic, New

York, 1974), Sec. 8.
[44]J. C. Tully, Phys. Rev. B **16**, 4324 (1977).
[45]K. S. Lam, T. F. George, and D. K. Bhattacharyya, Phys. Rev. A **27**, 1353 (1983).
[46]T. S. Wang and J. B. Delos, Phys. Rev. A **29**, 542 (1984); **29**, 552 (1984); **33**, 3832 (1986).
[47]F. Koike, J. Phys. B **20**, 1965 (1987).
[48]R. P. Feynman, Rev. Mod. Phys. **20**, 367 (1948); R. P. Feynman and A. R. Hibbs, *Quantum Mechanics and Path Integrals* (McGraw-Hill, New York, 1965).
[49]G. S. Agarwal, *Quantum Optics,* Vol. 70 of *Springer Tracts in Modern Physics,* edited by G. Höhler (Springer, Berlin, 1974).
[50]L. Allen and J. H. Eberly *Optical Resonance and Two-Level Atoms* (Wiley, New York, 1975).
[51]M. Lewenstein, J. Zakrzewski, T. W. Mossberg, and J. Mostowski, J. Phys. B **21**, L9 (1988).
[52]B. Fain, Phys. Rev. A **37**, 546 (1988).
[53]R. Zwanzig, Phys. Rev. **124**, 983 (1961).
[54]H. Mori, Prog. Theor. Phys. **33**, 423 (1965); **34**, 399 (1965).
[55]*Memory Function Approaches to Stochastic Problems in Condensed Matter,* Vol. 62 of *Advances in Chemical Physics,* edited by M. W. Evans, P. Grigolini, and G. Pastori Parravicini (Wiley, New York, 1985).
[56]J. N. Bardsley, A. Herzenberg, and F. Mandl, Proc. Phys. Soc., London **89**, 321 (1966).
[57]A. Herzenberg, J. Phys. B **1**, 548 (1968).
[58]W. H. Miller, J. Chem. Phys. **52**, 3563 (1970).
[59]M. Berman, L. S. Cederbaum, and W. Domcke, J. Phys. B **16**, 875 (1983).
[60]J. N. Bardsley and J. M. Wadehra, J. Chem. Phys. **78**, 7227 (1983).
[61]L. S. Cederbaum and W. Domcke, J. Phys. B **14**, 4665 (1981).
[62]C. Mündel and W. Domcke, J. Phys. B **17**, 3593 (1984).
[63]W. Domcke, L. S. Cederbaum, and F. Kaspar, J. Phys. B **12**, L359 (1979).
[64]W. Domcke and L. S. Cederbaum, J. Phys. B **13**, 2829 (1980).
[65]W. Domcke and L. S. Cederbaum, J. Phys. B **14**, 149 (1981).
[66]W. Domcke, J. Phys. B **14**, 4889 (1981).
[67]W. Domcke, J. Phys. B **16**, 359 (1983).
[68]H. Estrada and W. Domcke, J. Phys. B **18**, 4469 (1985).
[69]F. Koike, J. Phys. Soc. Jpn. **39**, 1590 (1975).
[70]E. P. Wigner, Phys. Rev. **73**, 1002 (1948).
[71]*Handbook of Mathematical Functions,* edited by M. A. Abramowitz and I. A. Stegun (Dover, New York, 1965).
[72]W. Furmanski and R. Petronzio, Nucl. Phys. B **195**, 237 (1982).
[73]G. P. Ramsey, J. Comput. Phys. **60**, 97 (1985).
[74]M. L. Goldberger and K. M. Watson, *Collision Theory* (Wiley, New York, 1964), Sec. 8.
[75]G. J. Schulz, Rev. Mod. Phys. **45**, 423 (1973).
[76]S. F. Wong, J. A. Michejada, and A. Stamatovic (unpublished); cited in Ref. 79.
[77]M. Allan, J. Phys. B **18**, 4511 (1985).
[78]D. T. Birtwistle and A. Herzenberg, J. Phys. B **4**, 53 (1971).
[79]L. Dubé and A. Herzenberg, Phys. Rev. A **20**, 194 (1979).
[80]I. S. Elets and A. K. Kanzanskii, Zh. Esksp. Theor. Fiz **80**, 982 (1981) [Sov. Phys.—JETP **53**, 499 (1981)].
[81]L. A. Morgan, J. Phys. B **19**, L439 (1986).
[82]M. Tronc, A. Huetz, M. Landau, F. Pichou, and J. Reinhardt, J. Phys. B **8**, 1160 (1975).
[83]D. Teillet-Billy and F. Fiquet-Fayard, J. Phys. B **10**, L111 (1977).
[84]G. W. Ford, M. Kac, and P. Mazur, J. Math. Phys. **6**, 504 (1965).
[85]P. Ullersma, Physica **32**, 27 (1966).
[86]H. Dekker, Phys. Rep. **80**, 1 (1981).
[87]M. A. Morrison, Phys. Rev. A **25**, 1445 (1982).
[88]B. L. Whitten and N. F. Lane, Phys. Rev. A **26**, 3170 (1982).
[89]K.-H. Kochem, W. Sohn, N. Hebel, K. Jung, and H. Ehrhardt, J. Phys. B **18**, 4455 (1985).
[90]R. G. Newton, *Scattering Theory of Waves and Particles* (McGraw-Hill, New York, 1966), Sec. 17.2.